AUTOMATED CIRCUMFERENTIAL MAPPING OF MENISCAL EXTRUSION FROM RMPRS USING SAM2 AND NNUNETV2

Ike Vayansky[1,2], Faysal Altahawi[1], Ahmet H. Ok[1], Richard Lartey[1], Nancy Obuchowski[1], Xiaojuan Li[1], Carl S. Winalski[1]
[1]Cleveland Clinic, Cleveland, OH; [2]Cleveland State University, Cleveland, OH
vayansi@ccf.org

DISCLOSURES: Ike R. Vayansky (N), Faysal Altahawi (N), Ahmet Hakan Ok (N), Richard Lartey (N), Nancy Obuchowski (3B-RSNA's QIBA; 5-Siemens, QURE, Takeda), Xiaojuan Li (3C-Siemens; 7B-Osteoarthritis and Cartilage, Magnetic Resonance in Medicine), Carl S. Winalski (4-Pfizer, Viatris; 8-Editorial Board - Osteoarthritis and Cartilage).

INTRODUCTION: Meniscal extrusion varies circumferentially and may be underestimated when measured on standard coronal/sagittal imaging. Radial multiplanar reconstructions (rMPRs) from 3D knee MRI enable region based circumferential mapping of extrusion measurements. We extend our rMPR extrusion mapping to near root-to-root coverage using two automated measurement pipelines. Automated measurements are compared against the average measurements of three readers from a prior study on manual reader reliability on the same patient cohort. Our objective is to establish a clinical workflow for automatically mapping meniscal extrusion around the full circumference of the meniscus, to quantify the level of agreement and reproducibility of automated circumferential extrusion mapping when compared to manual readers, and to validate a method for rapid analysis of a larger patient cohort.

METHODS: This study was approved by the local IRB and informed consent was provided by all patients. Twenty patients (n=20; 9 male, 11 female) from the MOON (Multicenter Orthopedic Outcomes Network) cohort with bilateral knee MRIs 10 years post-unilateral ACL reconstruction. Patients were randomly selected for (1) no tear, no extrusion, (2) tear, extrusion, (3) no tear, extrusion, and (4) tear, no extrusion status based on MOAKS (MRI Osteoarthritis Knee Score) assessment. Each group included a mix of operative (n=10) and non-operative (n=10) cases across groups. 40 menisci (20 medial, 20 lateral) from 3D SPACE fast spin echo (FSE) knee MRI were used to generate rMPRs centered in each meniscus from 60° to 300° at 1° increments (241 angles per meniscus, 9,640 rMPR slices total). For each meniscus and tibia, SAM2 was interactively prompted on the center angle (1 slice) and propagated bidirectionally to produce meniscus and tibia masks for all remaining angles. A single-fold 3D nnUNetv2 model was then trained on SAM2 labels to increase segmentation performance and boundary delineation of SAM2 labels. The nnUNetv2 model was then applied to all rMPRs to generate a second set of refined segmentation masks (Figure 1). Extrusion was defined as the distance from the tibial margin to the inferior-most peripheral meniscal boundary per angle, and automated measurements were computed from masks using a geometric based point selection method. This distance was then adjusted for pixel spacing in millimeters. Automated measurement pipelines are quantified by comparing: (1) Readers vs Readers (R-R) reliability using an existing 41-angle manually measured dataset (120°-240°, 3° step, 2 trained readers, 1 MSK radiologist); (2) Average Readers vs SAM2 (R-S) on the overlapping angles; (3) Average Readers vs nnUNetv2 (R-N) on the overlapping angles. Interreader reliability was assessed using intraclass correlation coefficient (ICC, 2-way random, absolute agreement), 95% reproducibility coefficient (RDC95), within-meniscus within-angle SD (WMWASD) averaged across angles. A polar plot to show the average of all automated medial and lateral measurements mapped around the edge of the meniscus (Figure 2).

RESULTS: Our dataset comprises 9,640 rMPR slices (40 menisci x 241 angles) with accompanying tibial/meniscal masks and measurements. Near-root angles may lack meniscal tissue and may not extend to the true root edge. Table 1 shows the angle averaged ICC, WMWASD, and RDC95 by side and overall, for R-R, R-N, and R-S. Angle-averaged R-R reliability across 120-240° was ICC = 0.88, WMWASD = 0.50mm, RDC95 = 1.37mm (medial: ICC = 0.88, RDC95 = 1.44mm; lateral: ICC = 0.85, RDC95 = 1.28mm). On overlapping angles, R-S agreement was ICC = 0.69, WMWASD = 0.92mm, RDC95 = 2.56mm; angle-averaged ICC was higher medially than laterally (0.72 vs 0.50). R-N agreement was ICC = 0.70, WMWASD = 0.88mm, RDC95 = 2.44mm; again, higher medially than laterally (0.74 vs 0.54). Circumferential mapping showed a larger dispersion of measurements near the roots (Figure 2).

DISCUSSION: Our study shows that automated circumferential mapping using SAM2 prompted propagation and nnUNetv2 segmentation trained on uncorrected SAM2 labels demonstrated substantial agreement with manual readers on overlapping angles with an overall ICC = 0.70. Table 1 shows training the nnUNetv2 improved performance using a single-fold and without corrections from ICC = 0.69 (SAM2) to ICC = 0.70 (nnUNetv2). SAM2 provided initial segmentation with minimal prompting and nnUNetv2 offered improvement once trained on SAM2 derived labels. Our manual results when compared with automatic results show room for improvement (R-R ICC = 0.88 vs R-S ICC = 0.72 vs R-N ICC = 0.70). WMWASD (0.92mm vs 0.88mm) and RDC95 (2.56mm vs 2.44mm) show better agreement with manual readers using the nnUNetv2 pipeline because a lower RDC95 and WMWASD is better. Future work will investigate ensembling multiple models to increase segmentation and measurement performance, test other point selection algorithms, expand the patient cohort, establish voxel-wise consensus ground truths with experts across the full meniscal circumference.

SIGNIFICANCE / CLINICAL RELEVANCE: Circumferential root-to-root rMPR mapping paired with automatic measurement can quickly quantify meniscal extrusion to specific compartments and enable region-based mapping for clinical reporting using a streamlined pipeline for medical research. Our work may support a large-scale, reproducible clinical assessment of mapped extrusion measurements to improve detection, risk stratification, and establish compartment mapped extrusion measurements as a potential biomarker for osteoarthritis.

Table 1. R-R (Reader vs Reader), R-S (Reader vs SAM2), and R-N (Reader vs nnUNetv2) Angle-Averaged by Side

	Reader vs Reader			Readers vs SAM2			Readers vs nnUNetv2		
Side	ICC	WMWASD (mm)	RDC95 (mm)	ICC	WMWASD (mm)	RDC95 (mm)	ICC	WMWASD (mm)	RDC95 (mm)
Medial	0.88	0.52	1.44	0.72	0.82	2.28	0.74	0.80	2.22
Lateral	0.85	0.46	1.28	0.50	1.00	2.78	0.54	0.95	2.63
Overall	0.88	0.50	1.37	0.69	0.92	2.56	0.70	0.88	2.44

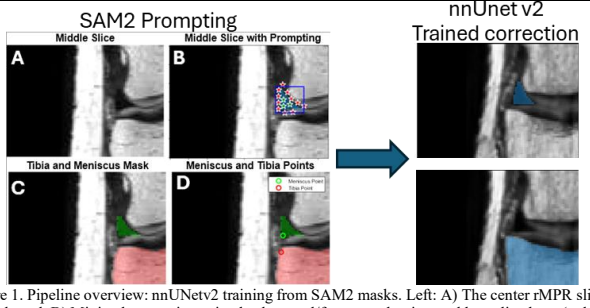

Figure 1. Pipeline overview: nnUNetv2 training from SAM2 masks. Left: A) The center rMPR slice is selected, B) Minimal prompting using background/foreground points and bounding box. (only meniscus prompting shown), C) Propagation of meniscal and tibial masks, D) Automatic point selection for meniscus and tibia on SAM2. Right: nnUNetv2 corrected mask.

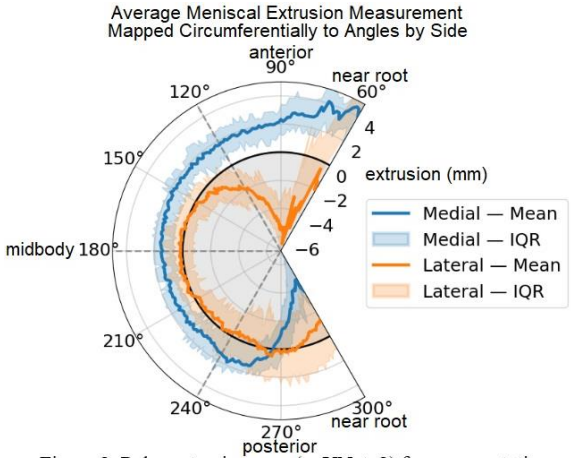

Figure 2. Polar extrusion map (nnUNetv2) for representative medial and lateral menisci.